Spectroscopic Study of Aqueous H$_2$SO$_4$ at Different Temperatures and Compositions: Variations in Dissociation and Optical Properties

Cathrine E. Lund Myhre,[†] **Daniel H. Christensen,**[‡] **Flemming M. Nicolaisen,**[‡] **and Claus J. Nielsen*,**[†]

Department of Chemistry, University of Oslo, P.O. Box 1033 Blindern, N-0372 Oslo, Norway, and Department of Chemistry, University of Copenhagen, Kemisk Lab. V, Universitetsparken 5, DK-2100 København, Denmark

The ionic speciation and the optical properties of aqueous H$_2$SO$_4$ have been investigated as a function of temperature and acid concentration by spectroscopic techniques. FT-Raman spectra have been obtained of 1.43−44.04 molal (12−81 wt %) aqueous H$_2$SO$_4$ in the temperature region from 300 to 220 K. The degree of dissociation of the second dissociation step in aqueous H$_2$SO$_4$ (α_2: HSO$_4^-$ ⇌ H$^+$ + SO$_4^{2-}$) is derived from the relative intensities of the HSO$_4^-$ Raman bands around 1050 cm^{-1} versus the SO$_4^{2-}$ band around 980 cm^{-1}, and a polynomial parametrization of α_2 is presented. FT-IR specular reflectance spectra are obtained of 6.46−44.04 molal (38−81 wt %) aqueous H$_2$SO$_4$ in the temperature region from 300 K to as far down as possible before crystallization by freezing occurred. The complex index of refraction is obtained from the IR reflectance spectra by the use of the Kramers−Kronig transformation, and the importance of including far-infrared data in the transformation is demonstrated. A revised parametrization of the density of aqueous sulfuric acid is given and an interpolation algorithm for obtaining the complex index of refraction of aqueous sulfuric acid solutions as a function of acid weight fraction and temperature is presented.

Introduction

The physical and chemical properties of the atmosphere are affected by the presence of aerosols,[1,2] and the formation of new aerosols is closely associated with the global climate and the greenhouse effect.[3] Aerosols act as sites for heterogeneous chemistry, and they have a significant direct impact on the radiative balance by scattering and absorption of solar radiation. In addition, the aerosols influence the radiative balance indirectly by acting as cloud condensation nuclei and thus affect the cloud microphysics and the albedo of the earth.[4,5] Sulfuric acid is a major component of tropospheric aerosols[6] and is also found throughout the lower and middle stratosphere.[7] The sulfate aerosols constitute the basis for the polar stratospheric clouds (PSC's) and are thereby linked to the stratospheric "ozone hole" chemistry in particular, and to the trace gas partitioning in general. The actual sulfate aerosol composition depends on the local partial water vapor pressure and the temperature, but in addition also upon the density, the surface tension, and the particle size through the Kelvin equation.[8]

Optical scattering techniques have commonly been used in satellite measurements of stratospheric aerosols.[9−14] Satellite observation is also an important source of information to understand the effects and the characteristics of tropospheric aerosols, such as optical depth, single scattering albedo, and size.[15−18] The complex index of refraction of the aerosol materials, $\bar{N}(\nu) = n(\nu) - ik(\nu)$, is a crucial and necessary parameter in the retrieval and interpretation of the remote sensing data[12−15,17−19] as the absorption and refractive index are fundamental parameters in the computation of the optical depth.

To model the radiative effect of atmospheric aerosols requires information on their size, spatial, temporal, and vertical distribution and knowledge of their optical properties. In turn, to calculate the optical properties of specific aerosols requires knowledge of the complex index of refraction together with the size distribution and normally also the density.[20,21]

We have previously presented results on the density and surface tension of sulfuric acid at low temperatures, allowing an accurate calculation of the overall composition of sulfuric acid aerosols as a function of size, water vapor pressure, and temperature.[22] Knowledge about the molecular and ionic constitution of aerosol material is needed to interpret the optical characteristics in terms of molecular and ionic properties. The present paper addresses two main issues, the ionic constitution of aqueous sulfuric acid and the complex index of refraction in the infrared spectral region.

Ionic Speciation in Aqueous Sulfuric Acid. There are several reviews of the thermodynamic properties of aqueous sulfuric acid. [23−26] There is, however, only one thermodynamic model that includes the dissociation of aqueous sulfuric acid in the whole concentration and temperature range relevant to the chemistry of the atmosphere.[26,27] The vibrational spectra of aqueous sulfuric acid were studied frequently until 25 years ago: detailed infrared[28−31] and Raman spectra[32] have been presented together with vibrational assignments. Infrared and Raman spectra of crystalline sulfuric acid have been published,[33] and more recently, low temperature infrared studies of sulfuric acid aerosols[34] and of solid sulfuric acid hydrides have been presented.[35−37] Results from infrared matrix isolation studies of sulfuric acid, including a complete vibrational assignment,[38] and of the complexes between sulfuric acid and water are also available.[39]

[†] University of Oslo.
[‡] University of Copenhagen.

Sulfuric acid dissociates in water in two steps:

$$H_2SO_4 + H_2O \rightleftarrows H_3O^+ + HSO_4^- \qquad (R1)$$

$$HSO_4^- + H_2O \rightleftarrows H_3O^+ + SO_4^{2-} \qquad (R2)$$
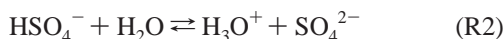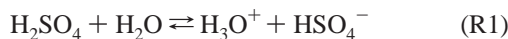
The degree of dissociation is described by the dissociation constants α_1 for the equilibrium R1 and α_2 for the equilibrium R2. Estimates of the degree of dissociation for the first step vary, but it is known to be very close to 1 in most concentration ranges. Infrared spectra show that dissociation to hydrogen sulfate is essentially complete already in solutions of ca. 40 molal acid (ca. 80 wt %).[30] Many studies have attempted to determine the degree of dissociation for the second step, α_2. The ionic constitution was derived from conductance measurements of dilute sulfuric acid solutions,[40] from ultraviolet spectroscopic studies,[41] from Raman measurements,[42–49] from measurements of apparent molar volumes,[50] from NMR studies,[51,52] and from studies by the cation-permselective membrane method.[53] Nearly all the studies were carried out at 25 °C; one Raman study reported the degree of dissociation at 0, 25, and 50 °C,[42] another Raman study reported results obtained at 15, 35, and 45 °C.[54]

Optical Constants of Aqueous Sulfuric Acid. Previous studies of the refractive and absorption index of aqueous sulfuric acid have, with few exceptions, been carried out at room temperature and with low spectral resolution.[55–58] Recently, extensive work has been reported by Niedziela et al.[59] and by Biermann et al.[61] Various experimental methods and calculation procedures have been employed to obtain the complex index of refraction and significant differences are apparent. The studies also vary widely with respect to wavenumber region, resolution, concentrations investigated, and temperature range.

Experimental Section

Sample Preparation. The sulfuric acid solutions were prepared from concentrated sulfuric acid of p.a. quality (96–98% in H_2O, Fluka) and distilled water. The D_2SO_4–D_2O solutions were prepared from concentrated D_2SO_4 (96–98% in D_2O, 99.5 atom % D, Fluka) and D_2O (99.96 atom % D, ISOTEC inc.). The compositions of the solutions were subsequently determined by titration before and after use. The other solutions were prepared from standard laboratory p.a. quality chemicals that were dried before use. The accuracy of the concentration in the individual sulfuric acid solutions and of the salt solutions was better than 0.2%.

Raman Experiments. The Raman spectra were obtained with a Bruker IFS 66 FTIR equipped with the FRA 106 FT-Raman module and using the 1064 nm line of a Nd:YAG laser for excitation. The samples were studied in capillary tubes of ca. 2 mm inner diameter; the low temperature samples were surrounded by a specially designed quartz Dewar and cooled by a stream of cold nitrogen.[62] The sample temperature was controlled to within ±0.5 K. The nominal resolution was 4 cm^{-1}, and the spectra resulted from 250, 500, or 1000 averaged interferograms. A 4-point apodization function was employed in the Fourier transformation. The spectra were corrected for the instrumental response function using a Tungsten lamp as a blackbody source and for the ν^4 scattering efficiency. The general background from water was subtracted from all the spectra. A few Raman spectra were obtained with a conventional DILOR RTI30 spectrometer using the 514.5 nm line of an argon ion laser for excitation.
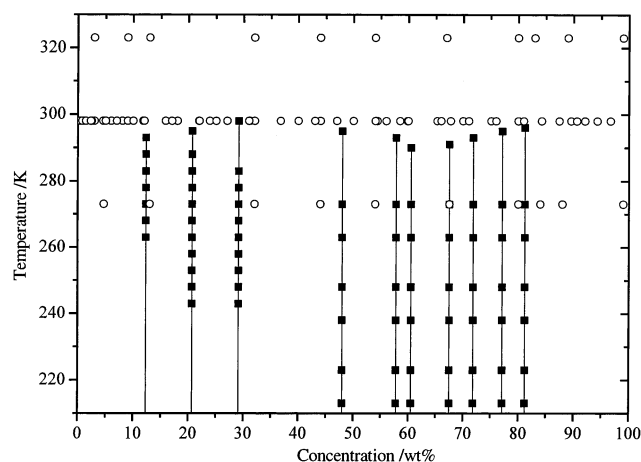

Figure 1. Map of the available measurements of the degree of dissociation of the second dissociation step in sulfuric acid: connected squares, this work; circles, previous data. See text.

Reflectance Measurements. Specular reflectance spectra of the 7500–400 cm^{-1} region were obtained with a Perkin-Elmer System 2000 FTIR spectrometer equipped with a room temperature DTGS detector and averaging 64 scans at a nominal resolution of 4 cm^{-1}. Far-infrared spectra (700–20 cm^{-1}) were obtained of room temperature samples with Bruker IFS113v (DTGS detector) and IFS HR120 instruments, the latter equipped with DTGS and He bolometer detectors. The optical setup was based on a standard specular reflection unit from Perkin-Elmer. A simple modification of the optical beam path allowed the surface of the sample support to be oriented horizontally, which made liquid surface studies feasible. The surface was studied by specular reflection at near normal incidence. To avoid getting a signal from the back of the sample, the equipment was designed for infinite thick samples; in the present case 25 mm was more than adequate.

A regulated stream of cold nitrogen cooled a specially developed temperature controlled sample holder. The temperature was controlled to within ±0.5 K, measured inside the samples, and the entire optical setup was enclosed in an environmental chamber. During the low temperature studies the chamber was purged with nitrogen to keep the relative humidity constant low and thereby prevent water vapor from condensing on the sample. Far-IR reflectance spectra were recorded for all the investigated concentrations. However, we did not have the possibility to measure the sulfuric acid solutions in the far-IR region at low temperatures. The low temperature mid-IR reflectance spectra were therefore extended by their corresponding far-IR spectra measured at room temperature.

The experimental specular reflectance spectra, $R(\nu)$, were obtained as a ratio of two single-beam spectra $I(\nu)$ and $I_0(\nu)$, where $I(\nu)$ is the intensity of the radiant flux reflected from the sample surface, and $I_0(\nu)$ is the intensity of radiant flux reflected from blank aluminized or gold plated mirrors, which exhibit constant reflectivity close to unity over the IR region under investigation.

Results and Discussion

Ionic Speciation in Aqueous H_2SO_4. The relative band intensities in the Raman spectra of aqueous sulfuric acid change substantially with acid weight fraction and, for a given sulfuric acid solution, also with the temperature. A total of 78 Raman spectra were recorded of aqueous H_2SO_4; the concentrations and temperatures of the samples studied are mapped in Figure 1. The effects in the spectra by changing the acid weight fraction
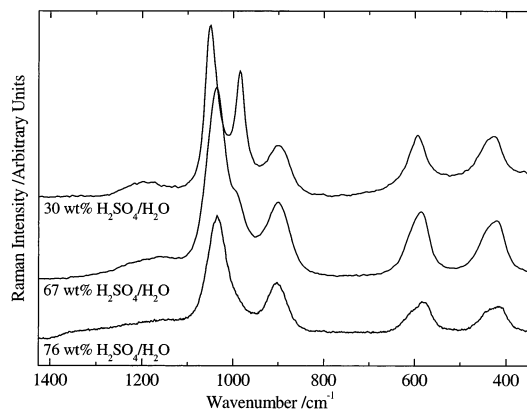
Spectroscopic Study of Aqueous H₂SO₄

J. Phys. Chem. A, Vol. 107, No. 12, 2003 **1981**

Figure 2. Raman spectra of three different concentrations of aqueous H_2SO_4 solution at room temperature.
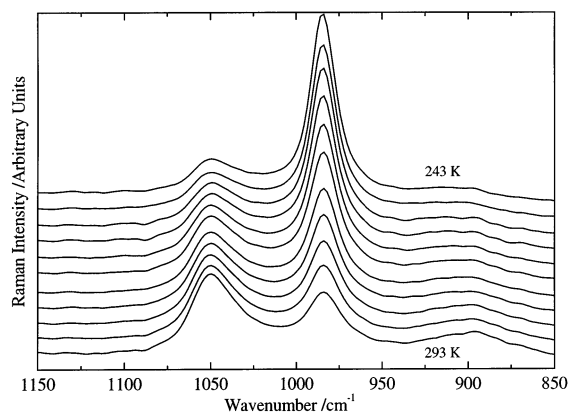

Figure 3. Raman spectra of a 29.1 wt % aqueous H_2SO_4 solution at 243 K (top) in steps of 5−293 K (bottom).
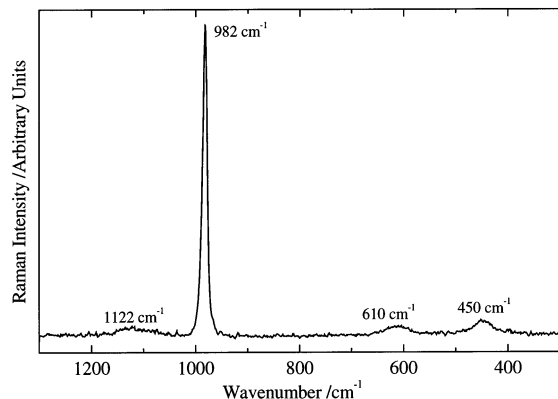

Figure 4. Raman spectrum of a saturated aqueous solution of Li_2SO_4. The spectrum is accurately fitted by four bands with Lorentz−Gaussian line shapes centered at 1122, 982, 610, and 450 cm^{-1}.

and the temperature are illustrated in Figures 2 and 3, respectively, and interpreted as a change in the degree of the second dissociation step, α_2. The Raman spectra contain overlapping bands from the sulfate and bisulfate ions. Hence, spectral deconvolution is needed to obtain the integrated intensities of the individual bands necessary to the calculation of the degree of dissociation, α_2.

Raman Spectra of the SO_4^{2-} Ion. The nine normal modes of vibration of the sulfate ion divide into $\Gamma_{vib} = 1a_1$ ($\sim$980 cm^{-1}) + 1e ($\sim$450 cm^{-1}) + 2f$_2$ ($\sim$1120, $\sim$610 cm^{-1}).[30] All fundamentals are Raman active; the f$_2$ modes are also infrared active. Figure 4 shows the Raman spectrum of a saturated aqueous Li_2SO_4 solution. As can be seen, the $\nu_1(a_1)$ band dominates the spectrum. The position of this band was reported to vary slightly
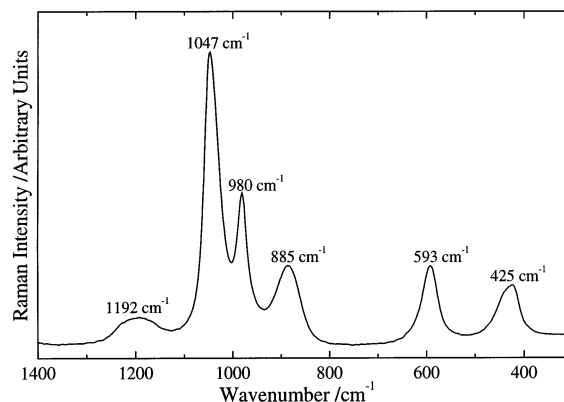

Figure 5. Raman spectrum of a saturated aqueous solution of (NH₄)-HSO₄. The spectrum is accurately fitted by seven bands with Lorentz−Gaussian line shapes centered at 1192, 1047, 1035, 980, 885, 593, and 425 cm^{-1}.

with the size of cation,[63] with the temperature,[64] and also with hydronium ion concentration.[65] Its half-width was reported to be independent of the viscosity[46] but to vary significantly with the hydronium ion concentration.[65−67] However, the integrated band intensity was reported to be independent of both cations present and the temperature.[63,64] To be discussed later, our observations for the aqueous sulfuric acid solutions confirm the variation in the line width with hydronium ion concentration.

The Raman spectrum of aqueous Li_2SO_4, Figure 4, can be accurately fitted by four bands with Lorentz−Gaussian line shapes centered on 1122, 982, 610, and 450 cm^{-1}, and with relative integrated intensity ratios of 0.123:1:0.234:0.324. The intensity ratios agree reasonably well with previous reported values for the $\nu_3(f_2)$ and $\nu_1(a_1)$ bands 0.187:1.[47] The molal scattering intensity of the $\nu_1(a_1)$ band relative to that of the $\nu_1(a_1)$ band in ClO_4^- is measured as 0.639 with a standard deviation of $\sigma = 0.011$ on the basis of five independent measurements. This is virtually the same ratio as reported by Dawson et al.[64] who studied the Raman spectrum of aqueous Na_2SO_4 solutions at elevated temperatures and also measured the integrated intensity of the 981 cm^{-1} (ν_1) line of SO_4^{2-} relative to the ν_1 band of ClO_4^-. They found that the integrated intensities showed very little variation with temperature and a relative molal scattering intensity of 0.637 with $\sigma = 0.015$.[64]

Raman Spectra of the HSO_4^- Ion. The twelve normal modes of vibration of the free hydrogen sulfate (bisulfate) ion with C_s symmetry divide into $\Gamma_{vib} = 8a' + 4a''$ with all modes being both Raman and infrared active. The Raman spectra of aqueous bisulfate solutions invariably contain bands from the sulfate ion as well. This is illustrated in Figure 5, showing the spectrum of a saturated aqueous solution of (NH₄)HSO₄ at 298 K in the 1500−300 cm^{-1} region. As can be seen, this part of the spectrum consists essentially of six bands, of which the broad feature with a maximum around 1192 cm^{-1} and the two peaks around 1047 and 885 cm^{-1} originate from HSO_4^-, the peak around 980 cm^{-1} is due to SO_4^{2-}, and the two peaks around 592 and 425 cm^{-1} arise from fundamental transitions of both ions; see above (the ammonium ion has no bands below 1400 cm^{-1}). The weak SO_4^{2-} band around 1110 cm^{-1} is hidden between and below the broad and much stronger 1192 and 1047 cm^{-1} HSO_4^- bands. In addition, the 1192 cm^{-1} feature likely contains a contribution from the H_3O^+ ion.[68] The 885 cm^{-1} band is reported to shift considerably in frequency with both temperature and concentration,[64] whereas the 1047 cm^{-1} band shifts in frequency with concentration and has a line width that increases with concentration.[69]

Ikawa and Kimura[65] studied the Raman band shapes of aqueous sulfuric acid and found that the $1100-850$ cm^{-1} region could be well approximated by a superposition of four Voight functions with peaks around 900, 980, 1030, and 1050 cm^{-1} at all concentrations between 0.5 and 10.6 M. A subsequent Raman study of bisulfate and sulfuric acid solutions reported that the asymmetry of the 1050 cm^{-1} band of HSO$_4^-$ could be reproduced by a band pair with identical line shapes and widths and reproduced where the weak component was centered 13 cm^{-1} lower that the main component.[67] It was also found that the integrated intensity of the two bands consistently was 1:0.18 for all the solutions studied; it was suggested that the weak component might originate from a hot band transition from the lowest bending vibration. To a first approximation, the relative intensity of such a hot band transition at 300 K would be ca. 12% of the fundamental. However, at 230 K it would only be ca. 6% and this may constitute a small systematic error in the intensity analysis; see later.

Irish and Chen[66] assumed Lorentz−Gaussian product line functions and identified an additional weak Raman line at 948 cm^{-1} in their computer analysis of bisulfate solutions. They attributed this band to the HSO$_4^-$ ion. In a later study they attributed the 948 cm^{-1} band to the ion pair H$_3$O$^+$SO$_4^{2-}$.[46] In another Raman study of aqueous sulfuric acid it was suggested that the 948 cm^{-1} band was fictitious and a result of the assumption of line shapes.[47] However, the asymmetry of the 1050 cm^{-1} band and the weak band around 1030 cm^{-1} were confirmed; the two bands were attributed to different forms of the hydrated HSO$_4^-$ ion. In a later paper Turner[47] restated that the alleged band at 948 cm^{-1} was a consequence of the Lorentz−Gaussian band shapes assumed by Irish and Chen.[66] The relative intensity of the HSO$_4^-$ band around 900 cm^{-1} to the 1050/1040 cm^{-1} pair was reported as 0.413:1.

In our deconvolution of the $1400-750$ cm^{-1} region we have constrained the wavenumber of the weak, broad ν_3 SO$_4^{2-}$ band at 1122 cm^{-1} and assumed the same relative intensity between the ν_3 and ν_1 bands of the SO$_4^{2-}$ ion, as found in the Li$_2$SO$_4$ solutions mentioned above. Introducing four additional HSO$_4^-$ bands centered around 1200, 1050, 1035, and 900 cm^{-1} was then both necessary and sufficient to fit the spectrum accurately.

Dawson et al.[64] studied the Raman spectra of (NH$_4$)HSO$_4$ solutions at elevated temperatures and measured the integrated intensity of the 1050/1040 cm^{-1} band pair of HSO$_4^-$ relative to the ν_1 band of ClO$_4^-$. They found that the relative integrated intensity showed very little variation with temperature and a relative molal scattering coefficient of 0.655, $\sigma = 0.013$ for HSO$_4^-$. We investigated four different mixtures of aqueous (NH$_4$)HSO$_4$/NaClO$_4$ solutions. The molal scattering intensity of the 1050/1040 cm^{-1} band pair relative to that of the ν_1(a$_1$) band of ClO$_4^-$ was measured as 0.676, and with standard deviation of $\sigma = 0.014$. That is, the present relative intensity measurements are in good agreement with the previously reported value.[64]

Raman Spectra of Aqueous H$_2$SO$_4$ Solutions. The 78 Raman spectra of $1.43-45.13$ molal $(12-81$ wt %) aqueous sulfuric acid have been analyzed in terms of the HSO$_4^-$ and SO$_4^{2-}$ ions only. For the higher concentrations there are, however, some indications of bands due to undissociated H$_2$SO$_4$.

We use the same procedure in the deconvolution of all the 78 Raman spectra: Five bands are needed to fit the spectra in the region $1400-750$ cm^{-1} accurately. Figure 6 shows an example of the deconvolution of a 29.1 wt % aqueous H$_2$SO$_4$ solution and has the bands centered around 1190, 1051, 1037,
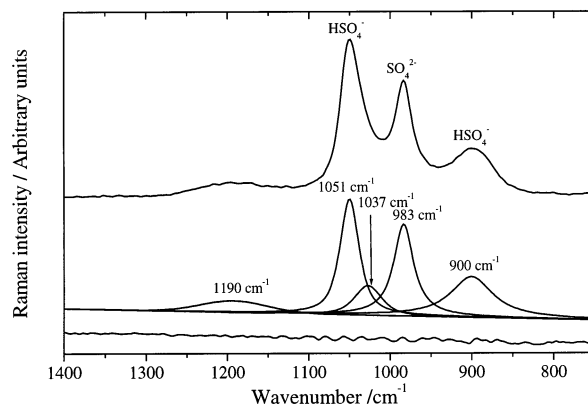

Figure 6. Raman spectrum of a 29.1 wt % aqueous H$_2$SO$_4$ solution at room temperature (top), the spectral deconvolution (middle), and the residual spectrum (bottom).
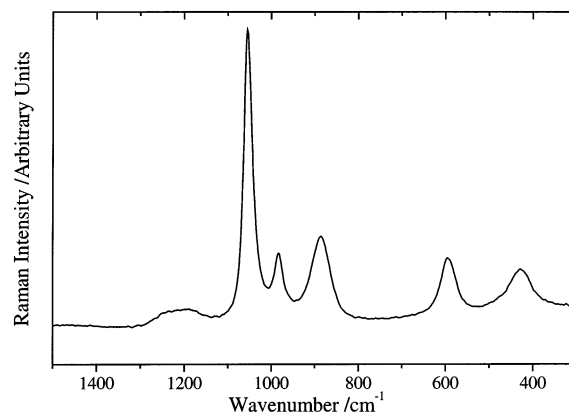

Figure 7. Raman spectrum of a 30 wt % D$_2$SO$_4$ in D$_2$O at room temperature.

983, and 900 cm^{-1}. The bands used in the analysis, 1051, 1037, and 983 cm^{-1}, and the 1190 cm^{-1} band are all accurately fitted by Lorentz line shapes whereas the band centered at 900 cm^{-1} is best fitted by a mixed Lorentz−Gaussian line shape. In the analysis of all the spectra, identical line widths of the two components in the 1050/1037 cm^{-1} pair are assumed, and their relative intensity is constrained to 1:0.18; see above. We have not been able to show any systematic variation in relative intensity of the two components with temperature.

The spectral deconvolution is obviously a critical point in the analysis. To elucidate the origin of the 1050/1040 cm^{-1} band pair of the bisulfate ion, we have also recorded Raman spectra of D$_2$SO$_4$−D$_2$O solutions. Figure 7 shows the Raman spectrum in the $1500-300$ cm^{-1} region of 4.19 molal (30 wt %) D$_2$SO$_4$ in D$_2$O. As can be seen, the spectrum closely resembles that of a similar H$_2$SO$_4$−H$_2$O solution. In particular, the asymmetry of the 1050 cm^{-1} band is evident. We tentatively apply the same constraints in the spectral decomposition of the D$_2$SO$_4$−D$_2$O spectra as applied in the analysis of the H$_2$SO$_4$−H$_2$O spectra. The position and relative intensity of the "1040 cm^{-1} band" to that of the "1050 cm^{-1} band" are strongly correlated. However, we find that the contour of the 1050/1040 cm^{-1} band in D$_2$SO$_4$−D$_2$O can be accurately reproduced using the same line width of the two components and the same relative intensity ratio of 1:0.18 as was reported for the H$_2$SO$_4$−H$_2$O system.[67] This result strongly supports the assumption that the two components of the 1050/1040 cm^{-1} band pair both have their origin in vibrations of the bisulfate ion alone.

Ionic Speciation of Aqueous H$_2$SO$_4$. The degree of dissociation of the bisulfate ion in aqueous sulfuric acid may be

TABLE 1: Integrated Relative Raman Scattering Intensities of the 1050/1040 and 980 cm⁻¹ Bands, and the Derived Values for the Degree of the Second Dissociation Step in Aqueous Sulfuric Acid, α_2

| H₂SO₄/H₂O | | | band intensity | | | H₂SO₄/H₂O | | | band intensity | | |
wt %	molal	temp/K	980 cm⁻¹	1050/1040 cm⁻¹	deg of dissociation, α_2	wt %	molal	temp/K	980 cm⁻¹	1050/1040 cm⁻¹	deg of dissociation, α_2
12.3	1.43	293	0.607	1.090	0.345	57.8	13.94	293	0.346	0.996	0.247
		288	0.700	1.059	0.385			273	0.461	0.856	0.337
		283	0.759	1.027	0.411			263	0.507	0.832	0.366
		278	0.840	1.071	0.426			248	0.627	0.774	0.434
		273	0.943	0.883	0.503			238	0.681	0.725	0.471
		268	1.032	0.785	0.554			223	0.772	0.651	0.529
		263	1.222	0.715	0.618			213	0.843	0.516	0.607
20.3	2.60	295	1.997	3.748	0.335	60.5	15.64	290	0.364	0.901	0.277
		288	2.383	3.168	0.416			273	0.413	0.823	0.322
		283	2.605	3.031	0.448			263	0.476	0.810	0.357
		278	2.767	2.934	0.471			248	0.581	0.755	0.421
		273	3.043	2.548	0.530			238	0.610	0.665	0.465
		268	3.306	2.382	0.568			223	0.655	0.572	0.520
		263	3.554	0.971	0.776			213	0.755	0.502	0.587
		258	3.091	1.491	0.662	67.5	21.18	291	0.345	1.125	0.225
		253	3.680	1.597	0.685			273	0.416	1.122	0.260
		248	4.489	1.544	0.733			263	0.423	1.121	0.263
		243	5.145	1.744	0.736			248	0.504	1.100	0.302
29.1	4.19	295	3.464	5.210	0.386			238	0.542	1.034	0.331
		288	3.830	4.905	0.425			223	0.591	0.952	0.370
		283	4.178	4.553	0.465			213	0.745	0.950	0.426
		278	4.428	4.445	0.485	71.8	25.96	290	0.396	1.446	0.206
		273	4.809	4.013	0.531			273	0.345	1.466	0.182
		268	5.434	3.907	0.568			263	0.391	1.488	0.199
		263	5.771	3.615	0.602			248	0.405	1.453	0.209
		258	6.037	3.317	0.633			238	0.459	1.374	0.240
		253	6.362	3.098	0.660			223	0.493	1.320	0.261
		248	6.509	2.803	0.687			213	0.552	1.256	0.294
		243	6.872	2.620	0.713	77.1	34.37	295	0.181	1.725	0.090
29.6	4.28	295	0.260	0.397	0.382			273	0.114	1.821	0.056
		273	0.309	0.242	0.547			263	0.130	1.615	0.071
		263	0.332	0.181	0.635			248	0.167	1.612	0.089
		248	0.398	0.139	0.730			238	0.191	1.678	0.097
		238	0.200	0.061	0.755			223	0.254	1.608	0.130
		223	0.146	0.022	0.861			213	0.291	1.599	0.147
		213	0.146	0.023	0.859	81.2	44.04	296	0.188	1.825	0.089
48.6	9.63	293	0.335	0.627	0.335			273	0.184	1.882	0.085
		273	0.387	0.515	0.415			263	0.183	1.828	0.087
		263	0.466	0.458	0.490			248	0.179	1.845	0.084
		248	0.509	0.382	0.558			238	0.216	1.830	0.100
		238	0.580	0.333	0.621			223	0.310	1.808	0.139
		223	0.456	0.130	0.768			213	0.345	1.743	0.158

calculated from the experimental spectra as

$$\alpha_2 = \frac{[SO_4^{2-}]}{[SO_4^{2-}] + [HSO_4^-]} = \frac{I_{SO_4^{2-}} \cdot S_{SO_4^{2-}}}{I_{SO_4^{2-}} \cdot S_{SO_4^{2-}} + I_{HSO_4^-} \cdot S_{HSO_4^-}}$$

(1)

where $I_{SO_4^{2-}}$ and $I_{HSO_4^-}$ are the integrated Raman scattered intensities of specific bands of the SO_4^{2-} and HSO_4^- ions, respectively, and $S_{SO_4^{2-}}$ and $S_{HSO_4^-}$ are the corresponding molal scattering coefficients (see above). As mentioned, the results from the D₂SO₄/D₂O studies show that the 1050/1040 band pair originates in vibrations of HSO₄⁻ alone. The integrated intensity of this band pair can therefore be used as a measure of the HSO₄⁻ concentration. The relative integrated Raman scattering intensities of the 1050/1040 cm⁻¹ HSO₄⁻ bands and the 980 cm⁻¹ HSO₄²⁻ band, as well as the derived values for the degree of dissociation, α_2, are presented in Table 1.

Young et al.[42] investigated 9 solutions at 273 K, 17 solutions at 298 K and 11 solutions at 325 K in the range of 2−95 wt % by Raman spectroscopy. In the samples with the highest concentrations, from ∼75 to 95 wt %, they observed indications of the presence of undissociated H₂SO₄. Due to difficulties with

overlapping bands these concentrations were therefore not included in their analysis of the degree of dissociation. To derive the ionic speciation, they first obtained a pseudo-absolute intensity of the 980 cm⁻¹ line of the SO₄²⁻ ion from a wide range of (NH₄)₂SO₄ solutions. They subsequently used this intensity−concentration proportionality to derive the HSO₄⁻ concentration from the stoichiometric concentration in (NH₄)-HSO₄ and sulfuric acid solutions.

Zarakhani and Vinnik[44] recorded Raman spectra of 0.1−1 acid weight fraction aqueous sulfuric acid at 25 °C but misinterpreted the spectra. Later Zarakhani et al.[45] repeated and extended their previous measurements and were able to derive concentration profiles for H₂SO₄, HSO₄⁻, and SO₄²⁻ as a function of acid concentration. To achieve internal consistency, they postulated a hydrate/ion pair with the composition H₂SO₄·H₂O. However, their concentration profile for H₂SO₄ is inconsistent with IR results.[30]

Chen and Irish[46] studied 18 solutions ranging from 0.025 to 0.81 weight fraction acid by Raman spectroscopy. Using the relative integrated intensity of the 980 cm⁻¹ line of the SO₄²⁻ ion, obtained from several bisulfate solutions,[66] they derived identical relative integrated intensities of the 1050 cm⁻¹ line of
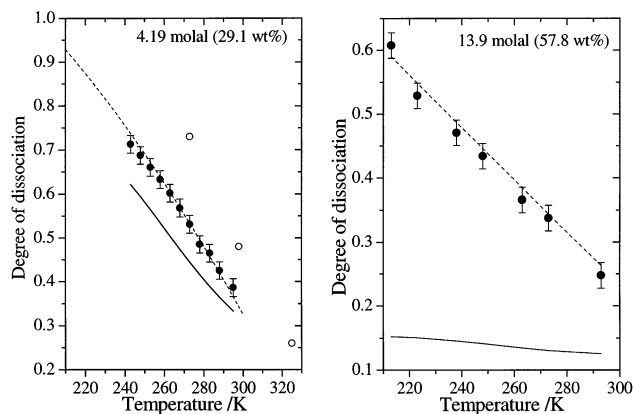
Figure 8. Degree of the second dissociation step, α_2, in different aqueous sulfuric acid solutions as a function of temperature. (●) This work. The error bars correspond to the rms value of the fit, 0.02. (○) Results from Young et al.[42] (—) Predictions of a multicomponent thermodynamic model.[26,27] (---) The model presented in this work.
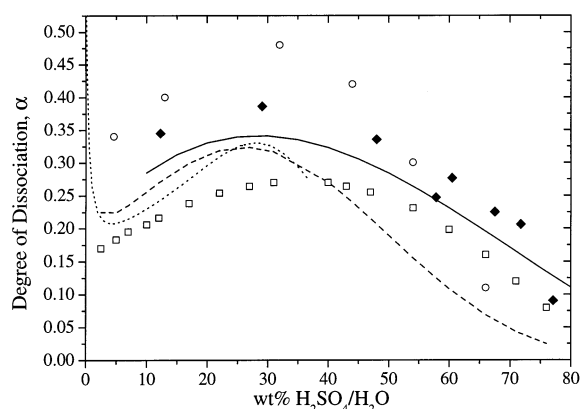

Figure 9. Degree of dissociation, α_2, of aqueous sulfuric acid at $T = 290-296$ K. Experimental results: (◆) this work; (○) results from Young et al.;[42] (□) results from Chen and Irish.[46] Model results: (—) predictions of the model presented in this work; (···) predictions of a multicomponent thermodynamic model by Clegg et al.;[25] (---) predictions of a multicomponent thermodynamic model by Clegg et al.[26]

the HSO_4^- ion in different sulfates and sulfuric acid solutions, as well as the degree of dissociation in sulfuric acid at 25 °C.

Cox et al.[48] analyzed 26 Raman spectra of aqueous sulfuric acid of 0.045−0.995 weight fraction acid employing chemometric methods. Their interpretation of the spectra included a hydrate/ion pair of composition $H_2SO_4 \cdot 2H_2O$; the analysis did not give quantitative information on the degree of dissociation. In a later paper Malinowski et al.[70] used 16 of the Raman spectra from the work of Cox et al.[48] and extended the analysis to give some semiquantitative information of the species present in the sulfuric acid solutions.

Recently, Tomikawa and Kanno,[71] presented results from a Raman study of sulfuric acid at +44 to −40 °C and interpreted the temperature dependence of the spectra in terms of a changing ionization of the acid. They show that the degree of the second dissociation step increases exponentially with decreasing temperature, but unfortunately, they only show some of their results in a graphical form.

The present derived ionic speciation is in good agreement with the predictions of a multicomponent thermodynamic model for the more dilute solutions,[26,27] whereas there is a substantial discrepancy for solutions of more than ca. 6.5 molal (ca. 40 wt %). This is illustrated in Figure 8, which also includes a few of the commensurate data of Young et al.[42] For all the solutions
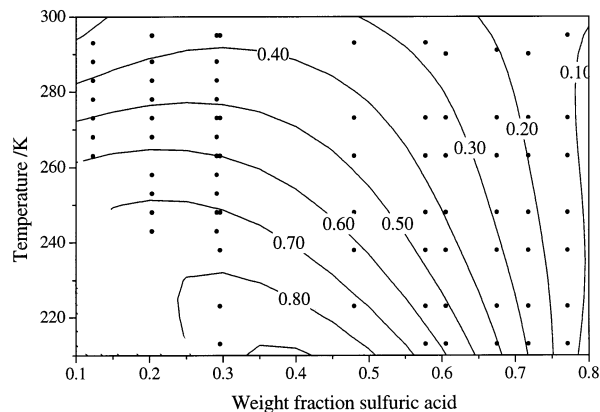

Figure 10. Contour plot of the calculated degree of dissociation in all the relevant (w, T) space. (●) (w, T) with experimental data from this work.

TABLE 2: Coefficients in the Polynomial Expansion of the Degree of Dissociation, α_2, of Aqueous Sulfuric Acid, $\alpha(w,T) = \sum_{i=0}^{3}\sum_{j=0}^{3}\alpha_{ij}w^i(T/\text{K} - 273.15)^j$

α_{ij}	$j = 0$	$j = 1$	$j = 2$	$j = 3$
$i = 0$	0.3933176	−0.0064027	−0.000026295	0.000000197
$i = 1$	1.2261331	−0.0128949		
$i = 2$	−2.9175425	0.0303050	0.0001422	
$i = 3$	1.1260874			

studied in the present work, and by Young et al.,[42] the degree of dissociation, α_2, increases with decreasing temperature; the largest temperature dependence is observed for solutions around 50 wt %.

Figure 9 compares the model predictions of Clegg et al.[26] for aqueous sulfuric acid solutions at 298 K to the experimental results of the present work and those of Young et al.[42] and Chen and Irish.[46] As can be seen, the data follow similar trends, but large deviations are evident between the different data sets. The explanation to this is complex, but the assignment and the deconvolution of the spectra is a determining factor in the experimental studies and, as described, this differs in the various experimental works. The model data of Clegg et al.[26] are based on various thermodynamic properties and, as the authors state, the speciation is not fully constrained by the thermal data alone. The predictive capability of their model with respect to the degree of dissociation is therefore to a certain extend biased by the range of, and the reliability of, the dissociation data included.

Parametrization of the Degree of Dissociation. To express the obtained degree of the second dissociation step, α_2, for all relevant concentrations and temperatures, we have performed an empirical parametrization. The complete set of the data was fitted to a polynomial function of the form

$$\alpha(w,T) = \sum_{i=0}^{3}\sum_{j=0}^{3}\alpha_{ij}w^i(T - 273.15)^j$$

where $\alpha(w,T)$ is the experimental degree of dissociation, w is the acid weight fraction, and T is the temperature in K. Needless to say, the coefficients α_{ij} have no physical significance. The coefficients are listed in Table 2. For the region 203 K $< T <$ 300 K and 10−75 wt %, the rms value of the fit is 0.02, and the agreement between experiment and model is satisfactory with deviations of less than 10%. Examples of the model predictions are shown for two concentrations in Figure 8. The parametrization is visualized in Figure 10: the degree of dissociation increases with decreasing temperature for all concentrations, and the largest temperature dependence is found
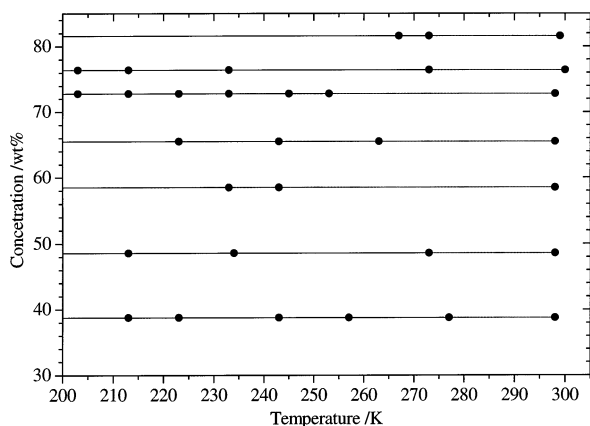
Spectroscopic Study of Aqueous H₂SO₄

J. Phys. Chem. A, Vol. 107, No. 12, 2003 **1985**

Figure 11. Map of the measured reflectance spectra of aqueous H$_2$SO$_4$.
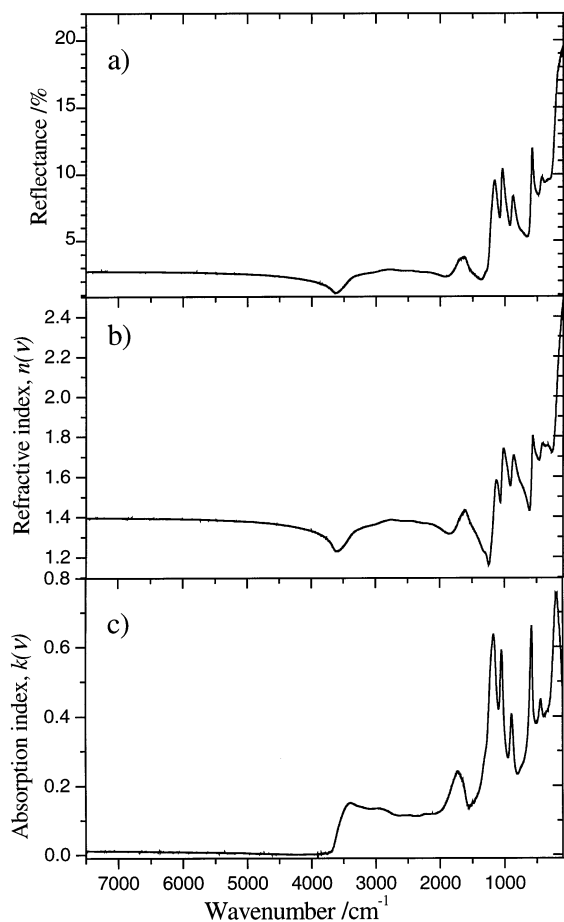

Figure 12. (a) Infrared specular reflectance spectrum (7500−20 cm^{-1}) of a 58.5 wt % aqueous sulfuric acid at T = 298 K. (b) Derived refractive index $n(\nu)$. (c) Derived absorption index $k(\nu)$.
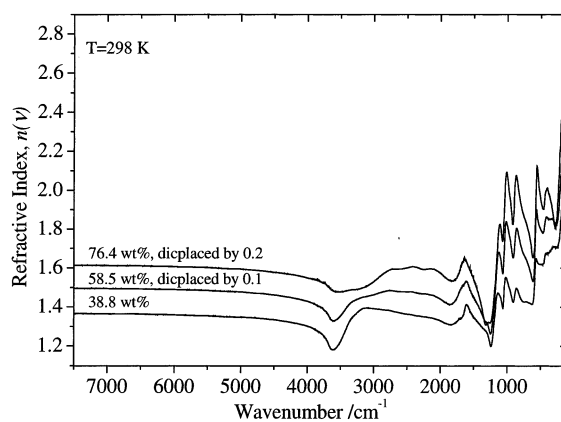

Figure 13. Refractive index of aqueous sulfuric acid at 298 K at different compositions.
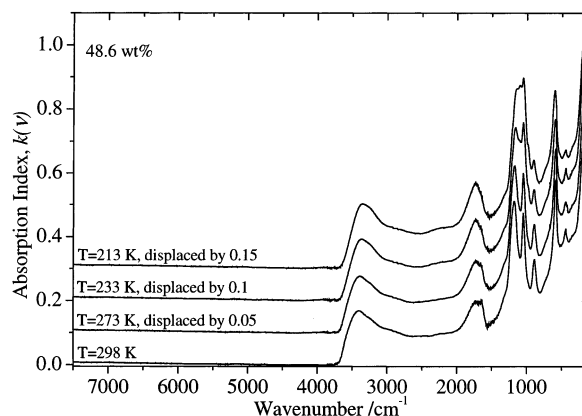
Figure 14. Absorption index of a 48.6 wt % aqueous sulfuric acid at different temperatures.

for concentrations around 40−50 wt %. The observed variations with temperature and concentration are paralleled by the variations in the surface tension for the system.[22,72] This agreement indirectly supports the validity of the spectral deconvolution as the surface tension is a thermodynamic property interpreted in terms of molecular interactions. It should be noted that Young and Grinstead[72] in their study of the surface tension of aqueous H$_2$SO$_4$ solutions interpreted the measured surface tension in terms of the pure components H$_2$SO$_4$, aqueous HSO$_4^-$, and aqueous SO$_4^{2-}$ in the system.

Optical Characterization of the Aqueous H$_2$SO$_4$ System. Specular reflectance IR spectra have been obtained of 6.46− 44.04 molal (38−81 wt %) aqueous H$_2$SO$_4$ solutions in the

temperature range 298−203 K. Figure 11 maps the 32 investigated compositions and temperatures. The complex index of refraction was calculated by use of the Kramers−Kronig transformation of the reflectance spectra. Figure 12 presents an example of a reflectance spectrum of a 58.5 wt % sulfuric acid together with the corresponding refractive index and absorption index. The reflectance spectra and the absorption and refractive index spectra change considerably with acid weight fraction and, for a given sulfuric acid solution, also with the temperature. Figure 13 demonstrates the concentration dependence of the refractive index at room temperature, and Figure 14 illustrates the temperature dependence of the absorption index of a 9.63 molal (48.6 wt %) sulfuric acid. The complete data set of optical constants is available through the journal as Supporting Information.

Application of the Kramers−Kronig Transformation. In general, the Kramers−Kronig analysis requires only a transmittance or a reflectance spectrum and the procedure can be applied to spectra with the origin in various kinds of techniques. There are two types of Kramers−Kronig analyses. One employs the Hilbert transformation of the absorption coefficient, $k(\nu)$, to the refractive index, $n(\nu)$; the other, used in this study, employs a transformation from reflectance, $R(\nu)$, to the phase shift, $\phi(\nu)$.[73,74] The relation between the response function and the absorption and refractive index, expressed in eqs 2−5 below, demonstrate the causality condition, and that an iterative procedure is necessary.

In the present work the complex index of refraction, $\tilde{N}(\nu) = n(\nu) - ik(\nu)$, was calculated from the experimental specular reflectance spectra at near normal incidence, $R(\nu)$. In the case of perpendicular incidence of light the boundary conditions give

the Fresnel's relation:

$$R(\nu) = \left[\frac{\bar{N}(\nu) - 1}{\bar{N}(\nu) + 1}\right]^2 \qquad (2)$$

The change of phase between the incident and reflected beam, $\phi(\nu)$, may be obtained by employing the Kramers–Kronig transformation:

$$\phi(\nu_m) = \frac{2\nu_m}{\pi} \int_0^\infty \frac{\ln(\sqrt{R(\nu)})}{\nu^2 - \nu_m^2} \, d\nu \qquad (3)$$

which enables one to calculate both $n(\nu)$ and $k(\nu)$ from $R(\nu)$:

$$n(\nu) = \frac{1 - R(\nu)}{1 + R(\nu) - 2\sqrt{R(\nu)} \cos(\phi(\nu))} \qquad (4)$$

$$k(\nu) = \frac{-2\sqrt{R(\nu)} \sin(\phi(\nu))}{1 + R(\nu) - 2\sqrt{R(\nu)} \cos(\phi(\nu))} \qquad (5)$$

The algorithm used in the present work is integrated in the Perkin-Elmer FT-IR spectrometer software.[75] The computations are based on the following assumptions: (i) the samples must be homogeneous, (ii) the specular reflectance beam must be measured at an angle of less than 10° from the perpendicular, and (iii) the sample must be thick enough to ensure that no light is reflected from the backside to prevent internal reflection effects. When aqueous solutions are studied, these assumptions are easily fulfilled for the infrared spectral region, as described in the Experimental Section. The algorithm also assumes that the spectral cutoff falls in a moderately flat unstructured region. This requirement rises from the evaluation of the integral (eq 3), and the implicit requirement of $R(\nu_\infty)$. In the low wavenumber region the condition of spectral flatness is not strictly fulfilled, and neglecting this can lead to large errors in the derived refractive and absorption index, see later.

The main advantage of using the Kramers–Kronig transformation from reflectivity, $R(\nu)$, to the phase shift, $\phi(\nu)$, compared to using absorption data, is that it does not require exact knowledge about the optical path length in the absorbing medium. Least-squares refinement calculations are also avoided.

To asses the precision and accuracy of the reflectance spectra and of the derived optical constants, $n(\nu)$ and $k(\nu)$, the experimental setup and the calculation procedure were tested using water as the standard. Several specular reflectance spectra of water were recorded in which the experimental conditions were varied randomly: the spectra were recorded on different days, new water samples were employed in each measurement, the optical equipment was taken out and remounted in the instrument, and the optical setup was deliberately misaligned and realigned. The average spectrum from 12 experiments obtained at 295–298 K showed a standard deviation below 0.3% reflectance over the whole wavenumber region, which leads to a precision in the refractive index of better than 1% and better than 3% in the absorption index. In addition, we also compared results obtained using different water qualities. The differences were negligible, in agreement with the findings of Bertie and Lan.[76]

Examination of the Kramers–Kronig Transformation. Bertie and Lan measured the complex index of refraction of water and reviewed the available data in the wavenumber region from 15000 to 1 cm^{-1}.[76] To inspect the Kramers–Kronig algorithm used in this work, and especially, the assumption that the spectral cutoff must fall in a moderately flat unstructured
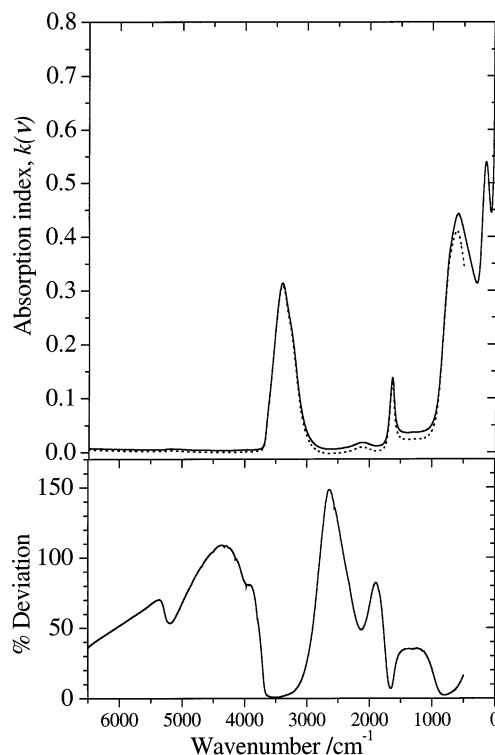

Figure 15. Influence of a low wavenumber spectral cutoff on the absorption, $k(\nu)$, index of water at 298 K calculated by the Kramers–Kronig transformation of a synthetic reflectance spectrum; see text. (—) Transformation based on the spectral range 6500–1 cm^{-1}. (···) Transformation based on the spectral range 6500–500 cm^{-1}. The percent deviation is included in the lower panel.

region, we constructed a synthetic reflectance spectrum of water from the refractive and absorption index spectra, $n(\nu)$ and $k(\nu)$, recommended by Bertie and Lan.[76] With this synthetic spectrum as the base, we explored the sensitivity of the computational procedure to high and low wavenumber spectral cutoff. The investigation showed that (1) the program retrieves the original absorption and refractive index when no spectral cutoff is employed; (2) the high wavenumber cutoff down to 5000 cm^{-1} has very little effect on the derived mid-IR absorption and refractive index; and (3) the low wavenumber cutoff has a significant impact on the derived absorption and refractive index, especially the absorption index. Figure 15 shows the absorption index resulting from two transformations in which the only difference lies in the low wavenumber cutoff. In case I (solid curve) the calculation was based on a reflectance spectrum including the far-IR region down to 1 cm^{-1}. In case II (dotted curve) the calculation was based on a typical mid-IR reflectance spectrum covering the region from 6500 to 500 cm^{-1}. The percent deviation between the derived indexes is included in the lower panel. For the absorption index one notices that the deviations are significant over a wide spectral range. Below 1600 cm^{-1} the differences vary between 3 and 50% and in the regions where the absorption index is small, the differences may reach several orders of magnitude. Regarding the refractive index, the difference is below 5% over the whole spectral region; in general, the refractive index is calculated smaller when the transformation is based on a wider wavelength region.

The investigation of the water system demonstrates the significance of the band structure in the spectral cutoff region. To minimize the above-mentioned systematic errors, we have therefore also collected reflectance spectra in the far-IR region (700–20 cm^{-1}) and in the near-IR region (10 000–5000 cm^{-1}). The importance of including the far-IR region seems to be even
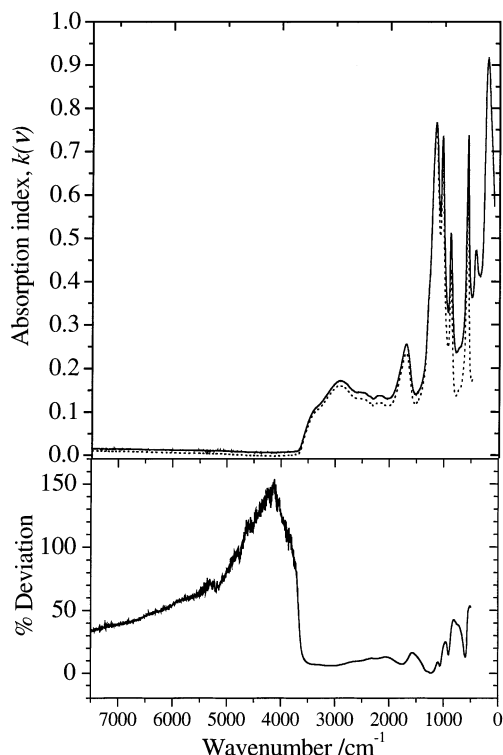
Figure 16. Influence of low wavenumber spectral cutoff on the refractive, $n(\nu)$, and absorption, $k(\nu)$, index of a 72 wt % aqueous sulfuric acid solution at 298 K calculated by the Kramers–Kronig transformation of a reflectance spectrum; see text. (—) Transformation based on the spectral range 7500–20 cm^{-1} (···) Transformation based on the spectral range 7500–500 cm^{-1}. The percent deviation is included in the lower panels.

more pronounced when the spectral structure has increased the complexity in the far-IR region. Figure 16 shows results for the 72 wt % sulfuric acid following the same calculation procedures as described above for water. Regarding the absorption index the deviations are as high as 20–50% in the band region and approximately 10% in the region from 4000 to 2000 cm^{-1} whereas the deviations in the refractive index are smaller, 0–10%.

From the above examination of the Kramers–Kronig transformation we recognize that neglecting the far-infrared part of the reflectance spectrum may lead to significant errors in the derived absorption and refractive index. For the refractive index the errors are small and mostly limited to the regions near the spectral cutoff. Considering the absorption index spectrum the errors can be large, 5–75%, and they are manifested in the entire spectrum, not only in the regions near the spectral cutoff. We also recognize that these errors/artifacts become larger as the low wavenumber spectral cutoff is moved to higher wavenumbers.

As mentioned, we have only recorded far-IR spectra (700–20 cm^{-1}) of the different samples at room temperature, which poses a principal problem. However, for all the samples studied the temperature variation of the 600–400 cm^{-1} region of the logarithm of the reflectance spectrum is essentially proportional to the variation in the sample density; see also "Interpolation of the optical data". Further, the Raman spectra of the low frequency region from 800 to 100 cm^{-1} show virtually no relative intensity variation among the bands as a function of temperature; the bands of H$_2$SO$_4$, HSO$_4^-$, and SO$_4^{2-}$ overlap completely in this region; see above. To a first approximation, one may assume a similar time dependency of the dipole and polarizability correlation functions, $\langle\mu(0)\cdot\mu(t)\rangle$ and $\langle\alpha(0)\cdot\alpha(t)\rangle$,

respectively. In turn, this leads to the fact that the logarithm of the far-IR reflectance spectrum (700–20 cm^{-1}) should show the same temperature dependence as the logarithm of the mid-IR reflectance spectrum (600–400 cm^{-1}). We may therefore to a first approximation extend the low temperature, mid-IR reflectance spectra by the properly scaled room temperature, far-IR reflectance spectrum of the same sample.

On the basis of the examination above, we estimate the uncertainty in our results to be within 2% for the refractive index and 3% for the absorption index, and that the uncertainties are mainly determined by the precision of the experimental specular reflectance spectra.

Comparison with Other Optical Infrared Data. A quick perusal of the optical infrared constants of aqueous sulfuric acid[56,60,61,77] shows significant differences among the data sets.

The data set of Palmer and Williams[56] has in some way been used as a reference or standard in the computation procedures in all of the later studies.[59–61,77] Palmer and Williams studied six different concentrations in the interval 25–96.6 wt % at 300 K and based their results on a combination of reflection measurements at near normal incidence and on transmittance studies. They used a spectral resolution of 20 cm^{-1}, applied the reflection technique in the spectral regions 28 000–14 000 cm^{-1} and 4000–400 cm^{-1}, and transmission measurements in the 14 000-4000 cm^{-1} region. In the region most relevant to the present work, 4000–400 cm^{-1}, they found the absorption to intense to allow the preparation of sufficiently thin films. Instead they used the near-normal reflectance technique followed by the Kramers–Kronig phase-shift analysis. In the Kramers–Kronig calculation they therefore implicitly assumed a constant reflectivity at wavenumbers lower than 350 cm^{-1} and the value of $R(\nu_\infty)$ to be sufficiently well-known from their measurements in the near UV region. For the less-concentrated H$_2$SO$_4$ solutions they used water as the reference in place of a mirror in the region 2800–1000 cm^{-1}. This procedure consequently introduced the refractive index of water, which was taken from a previous study by Downing and Williams,[78] in the calculation of the refractive index of aqueous sulfuric acid. According to the critical review of Bertie and Lan,[76] the data for water of Downing and Williams[78] are lower than the recommended values, mainly as a result of the instrumental and computational limitations of the early 1970s.[76] The discrepancies are on the order of 3–5% in most of the relevant spectral region, but approaching 1000 cm^{-1} the discrepancy increases to about 10%.[76]

Figure 17 compares our data of a 48.6 wt % sulfuric acid at 298 K with the data of Palmer and Williams[56] for a 50 wt % solution at 300 K. The agreement is fair, with respect to the refractive index but an increasing difference is evident in the low wavenumber region approaching as much as 7% around their spectral cutoff at 400 cm^{-1}. The difference is even more pronounced for the absorption index where the present results are 5–15% larger than those of Palmer and Williams.[56] We suggest that this systematic error, and the fact that Palmer and Williams[56] assumed a constant refractivity below 350 cm^{-1} is the explanation to the observed difference between their data and the present results. In fact, the agreement between our and their results is almost perfect if we neglect the far-IR part of the reflectance spectrum in the Kramers–Kronig transformation.

In comparison with the data of Niedziela et al.[77] we find significant deviations for the absorption index, $k(\nu)$. The largest deviation is found for a 72.8 wt % solution at 223 K, but comparable deviations are found for other concentrations and temperatures as well. Niedziela et al.[59,77] reported the first results based on measurements of laboratory generated sulfuric acid
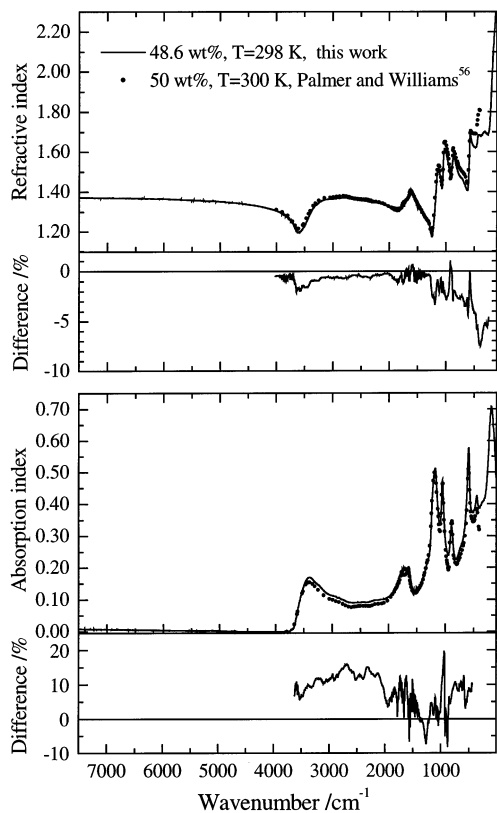
Figure 17. Comparison of the refractive and absorption index of a 48.6 wt % aqueous sulfuric acid at 298 K from this work (—) and a 50 wt % aqueous sulfuric acid at 300 K from Palmer and Williams[56] (···). The difference in percent is included in the respective lower panels.
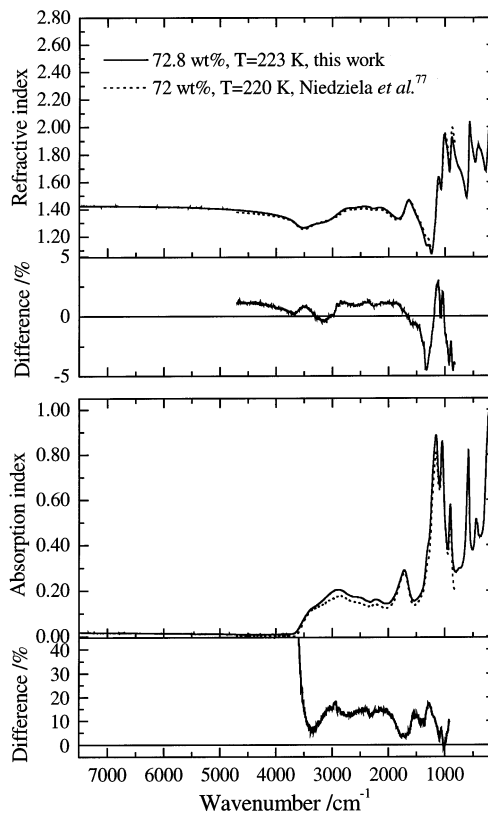
Figure 18. Comparison of the refractive and absorption index of a 72.8 wt % aqueous sulfuric acid at 223 K from this work (—) and a 72 wt % aqueous sulfuric acid at 220 K from Niedziela et al.[77] (···). The difference in percent is included in the respective lower panels.

aerosols. They measured 31 extinction spectra of sulfuric acid aerosols in the region 4700−825 cm^{-1} at 2 cm^{-1} resolution. After a detailed calibration process the composition of the aerosols were determined by measuring the water vapor pressure of the aerosol at equilibrium. The composition of the aerosol was in the range 32−85 wt % and the temperatures varied from 200 to 300 K. They used a subtractive Kramers−Kronig transformation in the calculation of $n(\nu)$ and $k(\nu)$, and their calculations were based on calculated anchor points at 3800 cm^{-1} for all the experimental spectra. The anchor points were estimated, using the Lorentz−Lorenz temperature correction to the data of Palmer and Williams[56] and interpolation and extrapolation from this data set. In the retrieval of optical parameters from aerosol extinction measurements it was also necessary for them to use Mie theory to obtain the refractive index. This implies an assumption of spherical particles smaller than the wavelength of the absorbed and reflected light beam, that is, $\lambda = 2.1−12.1$ μm. Niedziela et al.[59,77] did not present or comment on the size distribution used in their calculations.

Figure 18 compares the present results to the data of Niedziela et al.[77] for 72 wt % sulfuric acid at 220 K. Generally, the deviations appear to be the largest in band regions and in the regions near the spectral cutoff in the Niedziela et al. data set.[77] For the refractive index, $n(\nu)$, there is an acceptable agreement. However, the absorption index of Niedziela et al.,[77] is 10−20% lower than the present results. As above, we attribute these discrepancies to the fact that Niedziela et al.[77] only investigated the 4700−825 cm^{-1} region.

Biermann et al.[61] obtained their optical constants of aqueous sulfuric acid from studies of thin films. They made a systematic investigation in the region 5000−500 cm^{-1} of 13 concentrations from 10 to 96.6 wt % and temperatures in the interval 203−293 K. They first calculated $k(\nu)$ from the measured absorption.

In the next step they used the Kramers−Kronig relation to compute $n(\nu)$. Because they used thin films in their study, they also had to know the film thickness and this was calculated using the refractive index data of Palmer and Williams[56] and, again, the Lorentz−Lorenz correction and interpolation and extrapolation from this data set. They assumed a constant value for the absorption in the region above 5000 cm^{-1} and that the absorption decreased monotonically in the far-infrared region below 500 cm^{-1}.

A comparison between the present results and the data of Biermann et al.[61] is presented in Figure 19, and the disagreement is obvious. For the refractive index the deviations are up to 10% in the low wavenumber region, and the deviations in the absorption index are 5−25% and approaching 50% near their spectral cutoff in the low wavenumber region. We suggest that the deviations are due to their assumption of a monotonic decrease in the absorption in the far-infrared region. As our measurements demonstrate (see Figure 12), the reflectance of aqueous sulfuric acid actually increases in the far-infrared region.

Tisdale et al.[60] investigated eight concentrations of aqueous sulfuric acid near 215 K by measuring the transmittance of thin films and then employing the Kramers−Kronig analysis to obtain the refractive, $n(\nu)$, and absorption, $k(\nu)$, index. They assumed a value for the refractive index at infinite wavenumbers and that $k(\nu)$ was constant outside the 7000−500 cm^{-1} region. Further, they also had to estimate their film thickness. This required the density and the refractive index and they used the Lorentz−Lorenz temperature correction to the data of Palmer and Williams[56] and an interpolation and extrapolation of the concentrations and the corresponding densities. They used an iterative process involving both the calculation of the film thickness and the Kramers−Kronig transformation to obtain the optical constants. As a result they achieved the refractive index
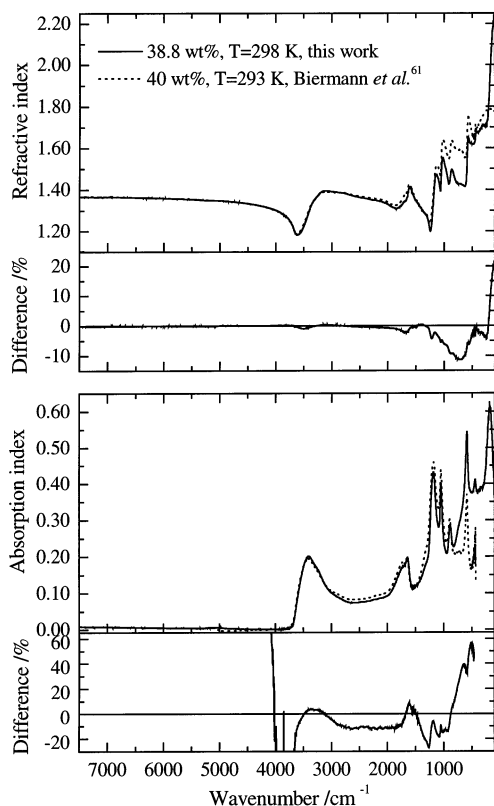
Figure 19. Comparison of the refractive and absorption index of a 38.8 wt % aqueous sulfuric acid at 298 K from this work (—) and a 40 wt % aqueous sulfuric acid at 293 K from Biermann et al.[61] (···). The difference in percent is included in the respective lower panels.
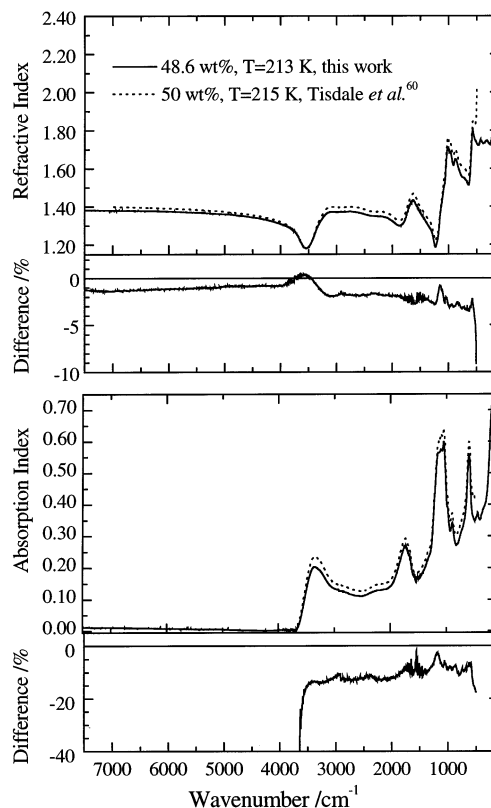

Figure 20. Comparison of the refractive and absorption index of a 48.6 wt % aqueous sulfuric acid at 213 K from this work (—) and a 50 wt % aqueous sulfuric acid at 215 K from Tisdale et al.[60] (···). The difference in percent is included in the respective lower panels.

for the region 7000−500 cm⁻¹ and the absorption index for the region 3650−500 cm⁻¹. Their results differ significantly from those of the earlier studies.[56,57] They explain the deviations by more than temperature differences and suggest errors in the reflection technique used in the earlier studies.[56,57] They recommend the use of their interpolated model data and not the measured values of the refractive and absorption indexes due to many sources of errors in their technique and measurements. Figure 20 shows a comparison between the data of Tisdale et al.[60] and the data from this work. The figure illustrates an acceptable agreement in the refractive index, but the absorption index is 10% too high compared to our data over the whole region 3650−500 cm⁻¹.

Interpolation of the Optical Data. A multivariate analysis was carried out to validate and to crosscheck the obtained optical data. The results showed that more than 98% of the variance could be explained by two principal components. Thus, a basis consisting of three pseudospectra should be adequate to span the whole weight fraction−temperature range covered by the experiments. The most intuitive approach, to us at least, is to interpret the optical parameters in terms of partial molar quantities. That is, in terms of the number of moles of HSO_4^-, SO_4^{2-}, H_3O^+, and H_2O per dm³. These concentrations depend on the density and the degree of the second dissociation step, α_2:

$$[HSO_4^-] = C_{o,SA}(1 - \alpha_2) \qquad [SO_4^{2-}] = C_{o,SA}\alpha_2$$

$$[H_3O^+] = C_{o,SA}(1 + \alpha_2) \qquad [H_2O] = C_{o,w} - C_{o,SA}(1 + \alpha_2)$$

$$C_{o,SA} = \frac{w\rho}{M_{SA}} \qquad\qquad C_{o,v} = \frac{(1 - w)\rho}{M_v}$$

where w is the sulfuric acid weight fraction, and ρ is the density. Obviously, the ionic concentrations are related, $[H_3O^+] = [HSO_4^-] + 2\cdot[SO_4^{2-}]$, and the absorption and refractive index spectra may therefore to a first approximation be described by the expressions:

$$n(\nu) = n_{HSO_4}(\nu)[SO_4^{2-}] + n_{SO_4}(\nu)[SO_4^{2-}] + n_{H_2O}(\nu)[H_2O]$$

$$k(\nu) = k_{HSO_4}(\nu)[SO_4^{2-}] + k_{SO_4}(\nu)[SO_4^{2-}] + k_{H_2O}(\nu)[H_2O]$$

As both the second dissociation step, α_2, and the density (see below), ρ, can be parametrized in terms of the sulfuric acid weight fraction, w, and the temperature, T, the spectra may also be indirectly parametrized in terms of the same two parameters.

The pseudospectra, resulting from a least-squares fit of the 29 experimental spectra, are available in tabular form through the journal as Supporting Information. For the region 203 K < T < 300 K and 38−75 wt % the agreement between the experimentally obtained complex index of refraction and the model is satisfactory. The deviations are generally less than 5% but increase to 10% in the regions where the dependence of temperature and concentration are the largest, that is, at low temperatures and low concentrations.

We have used a Mie scattering algorithm [79] to calculate the optical properties of sulfuric acid aerosols: the single scattering albedo, the asymmetry factor, and the specific extinction coefficient. The calculations were performed with a constant size distribution and the aerosols were assumed to be spherical. The results indicate that the variation in the optical aerosol properties due to *spectral* changes in the index of refraction with concentration and temperature is less than 20%. The Mie calculations also show that for the aqueous sulfuric water

TABLE 3: Coefficients in the Polynomial Expansion of the Density of Aqueous Sulfuric Acid, $\rho(w,T)/\text{kg}\cdot\text{m}^{-3} = \sum_{i=0}^{10}\sum_{j=0}^{3}\rho_{ij}w^i(T/\text{K} - 273.15)^j$

α_{ij}	$j = 0$	$j = 1$	$j = 2$	$j = 3$
$i = 0$	999.8426	334.5402×10^{-4}	-569.1304×10^{-5}	
$i = 1$	547.2659	-518.8577×10^{-2}	494.5427×10^{-4}	276.4890×10^{-7}
$i = 2$	526.295×10^1	280.7578×10^{-1}	-181.8361×10^{-3}	-238.7870×10^{-6}
$i = 3$	-621.3958×10^2	-188.7315	417.9279×10^{-3}	527.9089×10^{-6}
$i = 4$	409.0293×10^3	825.8149	-578.1934×10^{-3}	-475.173×10^{-6}
$i = 5$	-159.6989×10^4	-202.6090×10^1	431.4161×10^{-3}	161.0615×10^{-6}
$i = 6$	385.7411×10^4	275.8426×10^1	-133.2525×10^{-3}	
$i = 7$	-580.8064×10^4	-195.9292×10^1		
$i = 8$	530.1976×10^4	567.1429		
$i = 9$	-268.2616×10^4			
$i = 10$	576.4288×10^3			

system, variations in the density have a larger influence on the optical properties than the *spectral* variations in the index of refraction. The retrieval model presented above for calculation of $k(\nu)$ and $n(\nu)$ at relevant concentrations and temperatures reproduce the experimental values for a given temperature and concentration within $5-10\%$. The sensitivity test therefore suggests that the retrieval algorithm for the index of refraction is acceptable for most radiative transfer model purposes.

During the analysis we were made aware that our previous tabulated parametrization of the sulfuric acid density[22] unfortunately contained errors resulting in minor inaccuracies at low temperatures. The following polynomial parametrization of the density of aqueous sulfuric acid was therefore employed for the $\{w,T|0.10-0.90; 273-323\}$ regime:

$$\rho(w,T) = \sum_{i=0}^{10}\sum_{j=0}^{3}\rho_{ij}w^i(T - 273.15)^j$$

where $\rho(w,T)$ are the tabulated[80] and experimental density data,[22] w is the weight fraction of acid, and T is the temperature in K. $\rho_{\text{o,o}}$ was taken as the density of standard mean ocean water at $0\,°C$, and the $\rho_{\text{o},j}$ coefficients were determined by fitting a polynomial to the tabulated densities of standard mean ocean water.[81] A quadratic polynomial is sufficient to fit the density of water from 0 to 40 °C with a maximum error of less than $0.15\ \text{kg m}^{-3}$ and an rms error of less $0.08\ \text{kg m}^{-3}$. Similarly, the coefficients $\rho_{i,\text{o}}$ were obtained from a polynomial fit to the density of sulfuric acid at 0 °C.[80] In this case a polynomial of degree 10 is needed to model the 0 °C data such that the largest deviation is less than $0.4\ \text{kg m}^{-3}$ (rms error $0.12\ \text{kg m}^{-3}$). The $\rho_{i,\text{o}}$ and $\rho_{\text{o},j}$ terms were subsequently constrained to the above-mentioned values during the global fit. The final parametrization containing 32 terms, shown in Table 3, is continuos and well behaved in all the sulfuric acid weight fraction−temperature regime $\{w,T|0.10-0.90; 210-323\}$ and reproduces the tabulated data from the International Critical Tables[80] within $0.5\ \text{kg m}^{-3}$, and 95% of the density data from Myhre et al.[22] to better than $1\ \text{kg m}^{-3}$.

Summary

A systematic study of the ionic speciation and the optical constants in the infrared spectral region of aqueous H_2SO_4 was performed over a wide range of temperatures and acid concentrations. The degree of dissociation of the second dissociation step in aqueous H_2SO_4 (α_2: $HSO_4^- \rightleftharpoons H^+ + SO_4^{2-}$) is derived from the Raman spectra and a polynomial parametrization of α_2 as function of temperature and concentration is presented. It is shown that the main absorption and refractive features of the system H_2SO_4/H_2O are determined by the ionic speciation and of the solution. It is further shown that the computation of the

complex index of refraction by the Kramers−Kronig transformation of reflectance spectra is very sensitive to assumptions regarding the spectral range of the initial experimental data. Neglect of the far-infrared spectral region may lead to errors as large as $50-75\%$ in the absorption index, and the error is manifested in a wide range of the resultant spectra.

A simple retrieval algorithm for the refractive and absorption index of aqueous sulfuric acid, based on three pseudospectra, and depending only on the acid weight fraction and the temperature is presented.

Supporting Information Available: Table 2, with the coefficients required to calculate the speciation of HSO_4^-, SO_4^{2-}, H_3O^+, and H_2O in aqueous sulfuric acid at different temperatures and concentrations. Table 3, containing the coefficients needed in the calculation of the density. The experimental absorption, refractive indexes, and the pseudospectra needed in a retrieval procedure are also available. The material is available free of charge via the Internet at http://pubs.acs.org.

References and Notes

(1) Ravishankara, A. R. *Science (Washington, D.C.)* **1997**, *276*, 1058.

(2) Andreae, M. O.; Crutzen, P. J. *Science (Washington, D.C.)* **1997**, *276*, 1052.

(3) Charlson, R. J.; Schwartz, S. E.; Hales, J. M.; Cess, R. D.; Coakley, J. A., Jr.; Hansen, J. E.; Hofmann, D. J. *Science (Washington, D.C.)* **1992**, *255*, 423.

(4) Twomey, S. A.; Piepgrass, M.; Wolfe, T. L. *Tellus, Ser. B* **1984**, *36B*, 356.

(5) IPCC. Climate Change 2001: The Scientific Basis. Contribution of Working Group I to the Third Assessment Report of the Intergovernmental Panel on Climate Change. Houghton, J. T., Ding, Y., Griggs, D. J., Noguer, M., van der Linden, P. J., Dai, X., Maskell, K., Johnson C. A., Eds.; Cambridge University Press: Cambridge, U.K., and New York, 2001.

(6) D'Almeida, G. A.; Koepke, P.; Shettle, E. P. A. *Atmospheric Aerosols: Global Climatology and Radiative Characteristics*; Deepak Publishing: Hampton, VA, 1991.

(7) Turco, R. P.; Whitten, R. C.; Toon, O. B. *Rev. Geophys. Space Phys.* **1982**, *20*, 233.

(8) Renninger, R. G.; Hiller, F. C.; Bone, R. C. *J. Chem. Phys.* **1981**, *75*, 1584.

(9) Rosen, J. M.; Kjome, N. T.; Oltmans, S. J. *Geophys. Res. Lett.* **1990**, *17*, 1271.

(10) Deshler, T.; Adriani, A.; Hofmann, D. J.; Gobbi, G. P. *Geophys. Res. Lett.* **1991**, *18*, 1999.

(11) Baumgardner, D.; Dye, J. E.; Gandrud, B. W.; Knollenberg, R. G. *J. Geophys. Res.−Atmos.* **1992**, *97*, 8035.

(12) Massie, Steven T.; Deshler, T.; Thomas, G. E.; Mergenthaler, J. L.; Russell, J. M. *J. Geophys. Res.—Atmos.* **1996**, *101*, 23007.

(13) Hayasaka, T.; Meguro, Y.; Sasano, Y.; Takamura, T. *Appl. Opt.* **1998**, *37*, 961.

(14) Hervig, M. E.; Deshler, T.; Russell, J. M., III. *J. Geophys. Res.—Atmos.* **1998**, *103*, 1573.

(15) Kaufman, Y. J.; Tanre, D.; Remer, L. A.; Vermote, E. F.; Chu, A.; Holben, B. N. *J. Geophys. Res.—Atmos.* **1997**, *102*, 17051.

(16) Husar, R. B.; Prospero, J. M.; Stowe, L. L. *J. Geophys. Res.—Atmos.* **1997**, *102*, 16889.

(17) Nakajima, T.; Higurashi, A. *Geophys. Res. Lett.* **1998**, *25*, 3815.

(18) King, M. D.; Kaufman, Y. J.; Tanre, D.; Nakajima, T. *Bull. Am. Meteorol. Soc.* **1999**, *80*, 2229.

(19) Russell, P. B.; Hobbs, P. V.; Stowe, L. L. *J. Geophys. Res.—Atmos.* **1999**, *104*, 2213.

(20) Claquin, T.; Schulz, M.; Balkanski, Y.; Boucher, O. *Tellus, Ser. B: Chem. Phys. Meteorol.* **1998**, *50B*, 491.

(21) Jacobson, M. Z. *J. Geophys. Res.—Atmos.* **2001**, *106*, 1551.

(22) Myhre, C. E. L.; Nielsen, C. J.; Saastad, O. W. *J. Chem. Eng. Data* **1998**, *43*, 617.

(23) Pitzer, K. S.; Roy, R. N.; Silvester, L. F. *J. Am. Chem. Soc.* **1977**, *99*, 4930.

(24) Zeleznik, F. J. *J. Phys. Chem. Ref. Data* **1991**, *20*, 1157.

(25) Clegg, S. L.; Rard, J. A.; Pitzer, K. S. *J. Chem. Soc., Faraday Trans.* **1994**, *90*, 1875.

(26) Clegg, S. L.; Brimblecombe, P. *J. Chem. Eng. Data* **1995**, *40*, 43.

(27) Carslaw, K. S.; Clegg, S. L.; Brimblecombe, P. *J. Phys. Chem.* **1995**, *99*, 11557.

(28) Giguere, P. A.; Savoie, R. *Can. J. Chem.* **1960**, *38*, 2467.

(29) Giguere, P. A.; Savoie, R. *J. Am. Chem. Soc.* **1963**, *85*, 287.

(30) Walrafen, G. E.; Dodd, D. M. *Trans. Faraday Soc.* **1961**, *57*, 1286.

(31) Stopperka, K. *Z. Anorg. Allg. Chem.* **1969**, *370*, 80.

(32) Gillespie, R. J.; Robinson, E. A. *Can. J. Chem.* **1962**, *40*, 644.

(33) Goypiron, A.; De Villepin, J.; Novak, A. *Spectrochim. Acta, Part A* **1975**, *31A*, 805.

(34) Anthony, S. E.; Tisdale, R. T.; Disselkamp, R. S.; Tolbert, M. A.; Wilson, J. C. *Geophys. Res. Lett.* **1995**, *22*, 1105.

(35) Horn, A. B.; Jessica Sully, K. *Phys. Chem. Chem. Phys.* **1999**, *1*, 3801.

(36) Nash, K. L.; Jessica Sully, K.; Horn, A. B. *Phys. Chem. Chem. Phys.* **2000**, *2*, 4933.

(37) Nash, K. L.; Sully, K. J.; Horn, A. B. *J. Phys. Chem. A* **2001**, *105*, 9422.

(38) Givan, A.; Larsen, L. A.; Loewenschuss, A.; Nielsen, C. J. *J. Mol. Struct.* **1999**, *509*, 35.

(39) Givan, A.; Larsen, L. A.; Loewenschuss, A.; Nielsen, C. J. *J. Chem. Soc., Faraday Trans.* **1998**, *94*, 827.

(40) Sherrill, M. S.; Noyes, A. A. *J. Am. Chem. Soc.* **1926**, *48*, 1861.

(41) Edward, J. T.; Wang, I. C. *Can. J. Chem.* **1965**, *43*, 2867.

(42) Young, T. F.; Maranville, L. F.; Smith, H. M. *Structure of Ectrolytic Solutions*; Hamer, Walter J., Ed.; John Wiley & Sons: New York, 1959; p 35.

(43) Young, T. F.; Walrafen, G. E. *Trans. Faraday Soc.* **1961**, *57*, 34.

(44) Zarakhani, N. G.; Vinnik, M. I. *Zh. Fiz. Khim.* **1963**, *37*, 503.

(45) Zarakhani, N. G.; Librovich, N. B.; Vinnik, M. I. *Zh. Fiz. Khim.* **1971**, *45*, 1733.

(46) Chen, H.; Irish, D. E. *J. Phys. Chem.* **1971**, *75*, 2672.

(47) Turner, D. J. *J. Chem. Soc., Faraday Trans. 1* **1974**, *70*, 1346.

(48) Cox, R. A.; Haldna, U. L.; Idler, K. L.; Yates, K. *Can. J. Chem.* **1981**, *59*, 2591.

(49) Haldna, U.; Cox, R. A.; Juga, R.; Rajavee, E. *Eesti NSV Tead. Akad. Toim., Keem.* **1987**, *36*, 261.

(50) Lindstrom, R. E.; Wirth, H. E. *J. Phys. Chem.* **1969**, *73*, 218.

(51) Hood, G. C.; Reilly, C. A. *J. Chem. Phys.* **1957**, *27*, 1126.

(52) Kostromina, N. A.; Anikina, N. S.; Vdovenko, I. D. *Ukr. Khim. Zh. (Russ. Ed.)* **1982**, *48*, 230.

(53) Wallace, R. M. *J. Phys. Chem.* **1966**, *70*, 3922.

(54) Zarakhani, N. G. *Zh. Fiz. Khim.* **1978**, *52*, 1954.

(55) Remsberg, E. E.; Lavery, D.; Crawford, B., Jr. *J. Chem. Eng. Data* **1974**, *19*, 263.

(56) Palmer, K. F.; Williams, D. *Appl. Opt.* **1975**, *14*, 208.

(57) Pinkley, L. W.; Williams, D. *J. Opt. Soc. Am.* **1976**, *66*, 122.

(58) Gosse, S. F.; Wang, M.; Labrie, D.; Chylek, P. *Appl. Opt.* **1997**, *36*, 3622.

(59) Niedziela, R. F.; Norman, M. L.; Miller, R. E.; Worsnop, D. R. *Geophys. Res. Lett.* **1998**, *25*, 4477.

(60) Tisdale, R. T.; Glandorf, D. L.; Tolbert, M. A.; Toon, O. B. *J. Geophys. Res⊙—Atmos.* **1998**, *103*, 25353.

(61) Biermann, U. M.; Luo, B. P.; Peter, T. *J. Phys. Chem. A* **2000**, *104*, 783.

(62) Miller, F. A.; Harney, B. M. *Appl. Spectrosc.* **1970**, *24*, 291.

(63) Dean, K. J.; Wilkinson, G. R. *J. Raman Spectrosc.* **1983**, *14*, 130.

(64) Dawson, B. S. W.; Irish, D. E.; Toogood, G. E. *J. Phys. Chem.* **1986**, *90*, 334.

(65) Ikawa, S.; Kimura, M. *Bull. Chem. Soc. Jpn.* **1976**, *49*, 2051.

(66) Irish, D. E.; Chen, H. *J. Phys. Chem.* **1970**, *74*, 3796.

(67) Ikawa, S.; Yamada, M.; Kimura, M. *J. Raman Spectrosc.* **1977**, *6*, 89.

(68) Falk, M.; Giguere, P. A. *Can. J. Chem.* **1957**, *35*, 1195.

(69) Turner, D. J. *J. Chem. Soc., Faraday Trans. 2* **1972**, *68*, 643.

(70) Malinowski, E. R.; Cox, R. A.; Haldna, U. L. *Anal. Chem.* **1984**, *56*, 778.

(71) Tomikawa, K.; Kanno, H. *J. Phys. Chem. A* **1998**, *102*, 6082.

(72) Young, T. F.; Grinstead, S. R. *Ann. N. Y. Acad. Sci.* **1949**, *51*, 765.

(73) Yamamoto, K.; Ishida, H. *Vibr. Spectrosc.* **1994**, *8*, 1.

(74) Yamamoto, K.; Masui, A. *Appl. Spectrosc.* **1995**, *49*, 639.

(75) Perkin-Elmer. *Spectrum v2.00* **1998**.

(76) Bertie, J. E.; Lan, Z. *Appl. Spectrosc.* **1996**, *50*, 1047.

(77) Niedziela, R. F.; Norman, M. L.; DeForest, C. L.; Miller, R. E.; Worsnop, D. R. *J. Phys. Chem. A* **1999**, *103*, 8030.

(78) Downing, H. D.; Williams, D. *J. Geophys. Res.* **1975**, *80*, 1656.

(79) Wiscombe, W. J. *Appl. Opt.* **1980**, *19*, 1505.

(80) *International Critical Tables of Numerical data, Physics, Chemistry and Technology*; McGraw-Hill: New York, 1928; p I.

(81) Marsh, K. N., Ed. *Recommended Reference Materials for the Realization of Physicochemical Properties*; International Union of Pure and Applied Chemistry, Blackwell: London, 1987.